

First access to β half-lives approaching the r-process path near $N=126$

T. Kurtukian-Nieto,^{1,*} J. Benlliure,¹ L. Audouin,² F. Becker,³ B. Blank,⁴ I.N. Borzov,^{3,†}
E. Casarejos,¹ M. Fernández-Ordóñez,¹ J. Giovinazzo,⁴ D. Henzlova,³ B. Jurado,³ K. Langanke,^{3,5}
G. Martínez-Pinedo,³ J. Pereira,¹ F. Rejmund,⁶ K.-H. Schmidt,³ and O. Yordanov³

¹*Universidad de Santiago de Compostela, E-15782 Santiago de Compostela, Spain*

²*Institut de Physique Nucléaire, F-91406 Orsay Cedex, France*

³*Gesellschaft für Schwerionenforschung mbH (GSI), Planckstr. 1, D-64291 Darmstadt, Germany*

⁴*CENBG - Université Bordeaux 1 - UMR 5797 CNRS/IN2P3,
Chemin du Solarium, BP 120, 33175 Gradignan Cedex, France*

⁵*Institut für Kernphysik, TU Darmstadt, Schlossgartenstr. 9, D-64289 Darmstadt, Germany*

⁶*GANIL, BP55025, F-14076 CAEN Cedex 5, France*

(Dated: August 13, 2021)

Heavy neutron-rich nuclei close to $N=126$ were produced by fragmentation of a 1 A GeV ^{208}Pb beam at the FRS at GSI. The β -decay half-lives of 8 nuclides have been determined. The comparison of the data with model calculations including an approach based on the self-consistent ground-state description and continuum QRPA considering the Gamow-Teller and first-forbidden decays provide a first indication on the importance of first-forbidden transitions around $A=195$. The measured data indicate that the matter flow in the r-process to heavier fissioning nuclei is faster than previously expected.

PACS numbers: 25.70.Mn, 27.80.+w, 23.40.-s, 21.10.Tg, 26.30.+k

The investigation of heavy neutron-rich nuclei in the laboratory has been a challenging problem during the last decades. In particular, the β -decay half-lives of nuclei on the astrophysical r-process path are of primary importance for the full understanding of this process [1]. They define how rapidly the heaviest nuclei are synthesized during the r-process, thus determining the strength of fission cycling [2]. Moreover, these half-lives define the matter-flow bottlenecks, which largely affect the r-process abundance pattern. However, the scarce experimental data on r-process nuclei, along with the large discrepancies between theoretical predictions which differ by orders of magnitude, contribute to the difficulties in understanding the astrophysical r-process. This is particularly true for the $N \approx 126$ region far below the doubly magic ^{208}Pb , which remains a practically unexplored territory. The half-lives of these nuclei determine the relative $A = 195$ r-process peak abundances as well as the matter flow to even heavier nuclei.

In general there exist two complementary methods for providing and for separating the nuclei of interest: the in-flight [3] technique and the isotope-separation on-line (ISOL) technique [4]. Both methods have extensively been used for β -decay studies of r-process-relevant nuclei at different regions of the chart of the nuclides (e.g. around ^{78}Ni [5] and ^{130}Cd [6]). The ISOL technique suffers from specific difficulties for heavy neutron-rich nuclei. Elements between Hf ($Z = 72$) and Pt ($Z = 78$) are difficult to extract from the production target due to their low volatility, and for neutron-rich isotopes of the adjacent heavier elements, the ISOL technique suffers from an overwhelming isobaric contamination of isobars with higher Z , which are produced with much higher

cross sections. Background suppression was achieved for ^{218}Bi [7] as a peculiar case, by combining resonant-laser ionization and the specific condition that the isotope of interest is longer lived than the unwanted species. But these conditions are not generally applicable.

The in-flight separation, which is used in the present work, is universal, offering the advantage of fast ($< 1\mu\text{s}$), highly efficient, chemistry-independent separation. By tuning the magnetic fields of the separator, it is possible to select the desired region on the chart of nuclides and to perform experiments focusing either on one nucleus or on a ‘cocktail’ with a controlled background. Contaminants due to the small fraction of inevitable secondary reactions, produced during the stopping process, can be eliminated by a further range selection at the implantation stage. As a consequence, the clean particle identification for each implanted nucleus permits the direct correlation of an individual fragment with its subsequent β decay on an event-by-event basis. Important progress has been obtained during the last years profiting from relativistic heavy-ion beams, which made it possible to explore reaction mechanisms leading to the production of heavy neutron-rich nuclei. Cold-fragmentation reactions [8] opened a field not accessible by fission and form the basis for the achievement of the present work.

The experiment, which aimed at exploring the production of heavy neutron-rich nuclei close to the neutron closed shell $N = 126$ and for measuring their β half-lives, was performed at the fragment separator FRS [9] at the Gesellschaft für Schwerionenforschung (GSI) in Darmstadt, Germany. A ^{208}Pb primary beam of 1 A GeV, delivered by the SIS18 heavy-ion synchrotron, was directed to a beryllium target at the entrance of the FRS.

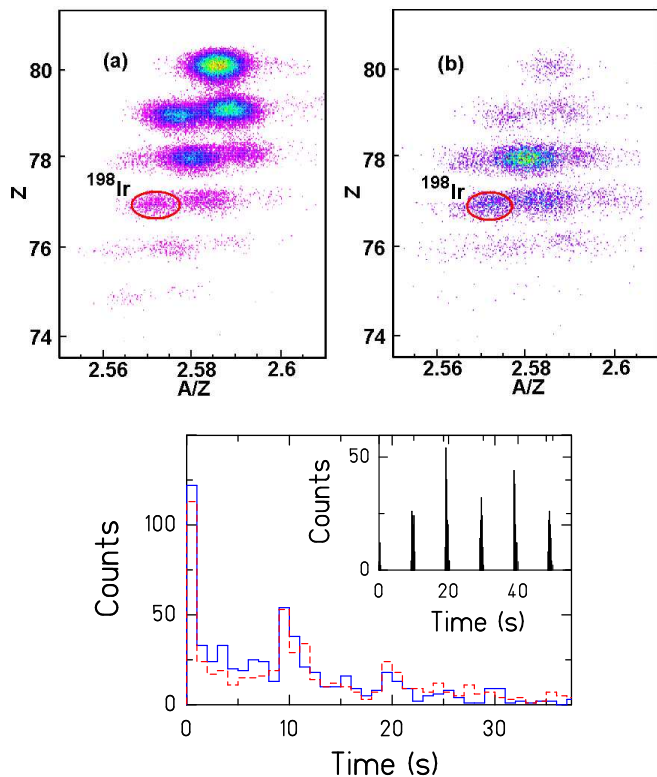


FIG. 1: (Color online). Top: Particle identification plots corresponding to a FRS setting optimized to transmit ^{198}Ir with a mono-energetic degrader. The figure shows the total production yield at the end of the FRS (a) and the ions which were implanted in the 1mm-thick DSSD (b). Bottom: Time-difference spectra between the ^{195}Re nuclei implanted and the first β -like event detected in the same strip, in forward- (solid line) and backward-time (dashed line). In the inset, the time structure of the beam is shown.

The reaction residues were identified by determining both their atomic number Z and their mass-over-charge ratio A/Z by means of the measurements of the energy loss, the magnetic rigidities, and the time of flight (ToF).

After leaving the FRS, the ions were slowed down to a few tens of A MeV in an aluminum plate and then implanted in an active stopper: a highly pixelated double-sided 1mm thick Si detector array (DSSD) with a surface of $20 \times 5 \text{ cm}^2$, covering the final image plane of the FRS. The use of a mono-energetic degrader at the FRS provided a large horizontal dispersion and a narrow range distribution of the fragments in the active stopper [10, 11]. The horizontal dispersion allowed taking advantage of the high pixelation of the active catcher to avoid multiple implantations of nuclei in the same pixel. The narrow range distribution of the fragments increased the implantation efficiency and allowed to implant several nuclides in a thin active stopper ($< 1 \text{ mm}$) at the same time. The identification plot of the nuclides leaving the FRS for a magnetic setting centred on ^{198}Ir is shown on the left upper part of Fig. 1. The correspond-

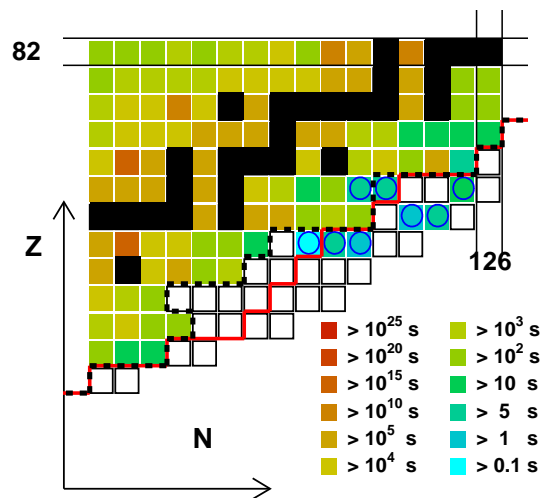


FIG. 2: (Color). Chart of the nuclides around $N = 126$. The color scale indicates the known β half-lives [13], while the circles correspond to the experimental values determined in this work. Empty boxes mark nuclei, identified in the present experiment, with no experimental half-life information available. The solid line denotes the limit of previously known nuclides and dashed line the limits of the known half-lives.

ing plot of the implanted nuclei in the right upper part of Fig. 1 demonstrates the additional selection by the implantation condition.

The half-lives of the nuclei were determined from position and time correlations between the implantation of the fully identified nuclei and the first β -like event observed after implantation, shown in the lower part of Fig. 1 for the case of ^{195}Re . We observed a beam-induced background in the recorded time-correlation spectra, originating from the time structure of the previously implanted nuclei and the presence of δ or atomic electrons generated during the beam pulse. The time structure of the beam, which is given by the periodic operation cycles of the synchrotron, is shown in the inset in the lower part of Fig. 1. In order to disentangle the background from the real events, the time differences between a given implantation and the previous β -like event was accumulated, shown in Fig. 1 by the dashed line. The ratio between the forward- and backward-time correlations, which decreases with time, contains the information on the ‘true’ fragment- β correlations.

In order to cope with the complex time structure in the present data, we developed a new method [12] to determine the β -decay half-lives: The experimental data were fitted with a numerical function (rather than an analytical function), obtained from Monte-Carlo simulations of time correlations between implantations and β -decay events, with the conditions found in the experiment. We performed sets of simulations with given values of β efficiency and lifetime, and we calculated the χ^2 from the measured and simulated ratios of the spectra

TABLE I: Measured β -decay half-lives compared with different model calculations.

Nuclide	$T_{1/2}$ (s)	DF3+QRPA (s)	Gr. Th. (s) [20]	FRDM (s) [19]
^{202}Ir	11_{-3}^{+3}	9.8	8.5	68.4
^{199}Ir	6_{-4}^{+5}	46.7	96.6	370.6
^{198}Ir	8_{-2}^{+2}	19.1	—	377.1
^{200}Os	6_{-3}^{+4}	6.9	16	187.1
^{199}Os	5_{-2}^{+4}	6.6	17.2	106.8
^{196}Re	3_{-2}^{+1}	1.4	5.1	3.6
^{195}Re	6_{-1}^{+1}	8.5	10.3	3.3
^{194}Re	$1_{-0.5}^{+0.5}$	2.1	16.1	70.8

of time correlations in forward and backward time for each set of simulations. This new analysis method solves a problem often arising in in-flight secondary-beam experiments when using conventional analysis tools, if the primary beam is delivered by a synchrotron.

In Table I we list the half-lives determined in this work with their uncertainties. Figure 2 shows the region of the chart of nuclides covered by the present work. The nuclear half-lives are indicated by the color scale, and the circles represent the half-lives measured in this work. We were able to synthesize more than 190 heavy neutron-rich nuclei ‘south’ of lead, 25 of which were identified for the first time.

The data of the new experiment do not extend to the extremely proton-deficient $N = 126$ nuclei on the r-process path ($Z \approx 65 - 72$). Therefore, r-process simulations still rely on theoretical models for the β -decay half-lives. These calculations have been done globally, i.e. for all r-process nuclei within the same framework, based on the Quasi-Particle Random Phase Approximation (QRPA) on top of macroscopic-microscopic mass models like the Finite Range Droplet Model (FRDM) [14] or the Extended Thomas Fermi with Strutinski Integral (ETFSI) approach [15], while Hartree-Fock-Bogoliubov (HFB) [16] and shell model [17] calculations have been reported for the $N = 126$ waiting point nuclei. However, the later two calculations considered only allowed Gamow-Teller (GT) transitions, while the work of Borzov [18], based on the continuum QRPA approach on top of mean-field ground states derived within the density-functional (DF) theory, includes the GT and first-forbidden (FF) transitions consistently within the same microscopic approach. This study gives strong evidence for important contributions of FF transitions to the total half-lives arising from $\nu 3p_{1/2} \rightarrow \pi 3d_{3/2}$ and $\nu 1i_{13/2} \rightarrow \pi 2h_{11/2}$ neutron-proton transitions and hence implies pure GT estimates of the half-lives of the $N = 126$ waiting points insufficient. As a consequence, FF transitions, however, derived within the statistical gross theory, have recently been added to the FRDM/QRPA approach

(noted FRDM in the following) [19]. Importantly the theoretical models predict noticeably different half-lives for the $N = 126$ waiting point nuclei making these input data for r-process simulations quite uncertain.

Although the nuclei studied here are not located on the r-process path, they are close enough to the $N = 126$ waiting points to serve as stringent tests for the theoretical predictions. In Table I we compare our measured half-lives with the prediction of the FRDM approach [19], the statistical ‘gross theory’ (Gr. Th.) [20] and a new microscopic calculation (DF3+QRPA) based on the Fayans energy-density functional. The later follows the half-life calculations for $N \sim 126$ nuclei as described in [18]. However, the strength functions for GT and FF transitions are calculated with no energy-dependent smearing. We stress that the DF3 functional used here describes the Q_β values of neutron-rich nuclei quite well [18]. Furthermore, the same approach has been proven to reproduce the measured half-lives of spherical nuclei in different regions of the nuclear chart ($Z = 20 - 30, N \approx 50$ [18], $Z = 42 - 49, N \approx 82$ [21]) quite well.

As can be seen in Table I, our DF3+QRPA model gives also a good account of the present half-lives, with the one exception of ^{199}Ir . The gross theory parametrization describes the data fairly well. On the other hand, the FRDM half-lives are for most nuclei more than one order of magnitude longer than the data. Fig. 3 compares half-lives from the FRDM and DF3+QRPA models for the Ir, Os and Re chains, including the $N = 126$ isotopes, and with data if available. For the odd-Z Re isotopes both models yield quite similar half-lives for the neutron-rich nuclei. However, both for the even-Z Os isotopes and odd-Z Ir isotopes the FRDM predicts substantially longer half-lives than the DF3+QRPA calculations and the available data. The consistently good agreement of the results of the spherical DF3+QRPA model with the presently reported half-lives, and with those in other regions of the nuclear chart, places some confidence in applying this approach also to the $N = 126$ r-process waiting points.

The calculated half-lives for the $N = 126$ isotones are shown in Fig. 4. Compared to the FRDM [19], which is often used in r-process simulations, the DF3+QRPA gives substantially shorter half-lives and does not show a pronounced odd-even staggering. Thus the break through the $N = 126$ waiting points, and hence the matter flow to the heavier fissioning nuclei [22], is faster. The GT contributions to the DF3+QRPA half-lives are very similar to those calculated with the shell model [17] and somewhat faster than the HFB results [16]. We note, however, that FF transitions, which speed up the half-lives (Fig. 4), are missed in the calculations of [16, 17].

In summary, an important step has been achieved in the study of new neutron-rich nuclei approaching the neutron closed shell at $N=126$. It has been shown that the $N=126$ region far below the doubly magic ^{208}Pb has be-

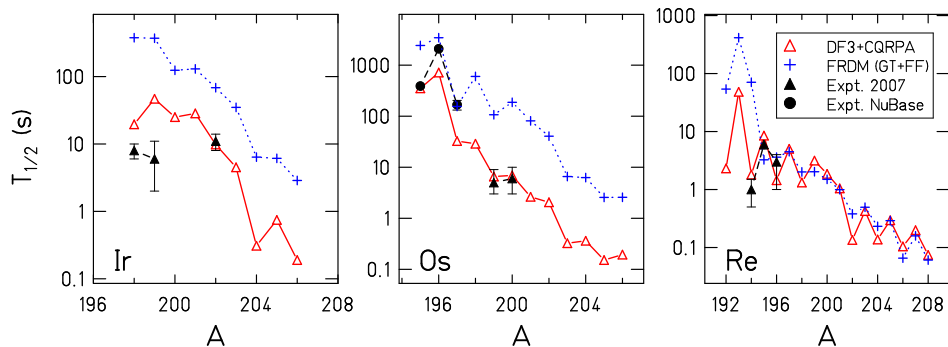


FIG. 3: (Color online). The total β -decay half-lives for Re, Ir and Os isotopic chains calculated within DF3+CQRPA in comparison with the ones from FRDM(GT+FF) [19], both with Gamow-Teller plus first-forbidden transitions. Filled triangles correspond to the experimental values measured in this work, circles (Os isotopes) to half-lives taken from literature [13].

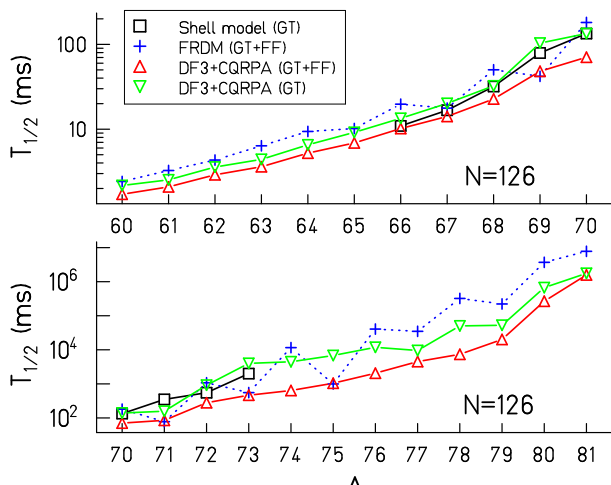


FIG. 4: (Color online). Calculated total β -decay half-lives for $N = 126$ isotones: triangles correspond to DF3+CQRPA calculations including only Gamow-Teller transitions (triangles-down) and Gamow-Teller plus first-forbidden transitions (triangles-up); Squares correspond to Shell-Model (GT) [17] calculations and crosses correspond to FRDM(GT+FF) half-life [19] calculations.

come accessible experimentally, and half-lives for nuclei reasonably close to the $N = 126$ r-process waiting points have been determined. Thus, for the first time data exist which put stringent constraints on the theoretical models required to calculate the half-lives of these r-process nuclei. We find that a comparison of the measured half-lives with those of a DF+QRPA calculation presented here is quite satisfactory, placing some confidence into the prediction of this model for the half-lives of the $N = 126$ r-process waiting-point nuclei. The calculations indicate significant contributions of first-forbidden transitions to the half-lives which have been either ignored or insufficiently accounted for in previous studies.

This work was supported by the Spanish MEC (FPA2005-00732), Xunta de Galicia (Consellería de Educación) and by the European Commission (EURONS,

contract no. 506065). I.N.B acknowledges the support by German DFG under the contract 436 RUS 113 907/0-1. T.K.-N. acknowledges the support from Xunta de Galicia, Dirección Xeral de Investigación, Desenvolvemento e Innovación (Bolsa Predoutoral, Consellería de Innovación e Industria) and Universidade de Santiago de Compostela, through the PhD studies.

* kurtukia@cenbg.in2p3.fr

† Present address: IPPE, Bondarenko Sq.1, 249033, Obninsk, Russia

- [1] J. J. Cowan et al., Phys. Rep. **208**, 267 (1991).
- [2] A. G. W. Cameron, The Astroph. J. **587**, 327 (2003).
- [3] D. Morrissey, B. M. Sherrill, Lect. Notes Phys. **651**, 113 (2004).
- [4] P. Van Duppen, Lect. Notes Phys. **700**, 37 (2006).
- [5] P.T. Hosmer et al., Phys. Rev. Lett. **94**, 112501 (2005).
- [6] K.-L. Kratz et al., Z. Phys. **A 325**, 489 (1986).
- [7] H. De Witte et al., Phys. Rev. **C 69**, 044305 (2004).
- [8] J. Benlliure, et al., Nucl. Phys. **A 660**, 87 (1999).
- [9] H. Geissel et al., Nucl. Instr. Meth. **B 70**, 286 (1992).
- [10] K.-H Schmidt et al., Nucl. Instr. Meth. **A 260**, 287 (1987).
- [11] C. Scheidenberger et al., Nucl. Instr. Meth. **B 204**, 119 (2003).
- [12] T. Kurtukian-Nieto et al., arXiv:nucl-ex/0711.0095 and to be submitted.
- [13] <http://www.nndc.bnl.gov/chart>.
- [14] P. Möller, J. R. Nix, and K.-L. Kratz, At. Data Nucl. Data Tables **66**, 131 (1997).
- [15] I.N. Borzov, Nucl. Phys. **A 688**, 382 (2001).
- [16] J. Engel et al., Phys. Rev. **C 60**, 014302 (1999).
- [17] K. Langanke and G. Martínez-Pinedo, Rev. Mod. Phys. **75**, 819 (2003).
- [18] I.N. Borzov, Phys. Rev. **C67** 025802 (2003).
- [19] P. Möller, B. Pfeiffer and K.-L. Kratz, Phys. Rev. **C 67**, 055802 (2003).
- [20] T. Tachibana, et al., Prog. Theor. Phys. **84**, 641 (1992).
- [21] I.N. Borzov et al., to be submitted.
- [22] G. Martínez-Pinedo et al., Prog. Part. Nucl. Phys. **59**, 199 (2007)